Polo kinase mediates the phosphorylation and cellular localization of Nuf/FIP3, a Rab11 effector

Lotti Brose[a,†], Justin Crest[a,b,†], Li Tao[a,c,*], and William Sullivan[a,*]
[a]Department of Molecular, Cell, and Developmental Biology, University of California, Santa Cruz, Santa Cruz, CA 95064; [b]Department of Molecular and Cell Biology, University of California, Berkeley, Berkeley, CA 94720; [c]Department of Biology, University of Hawaii, Hilo, HI 96720

ABSTRACT Animal cytokinesis involves both actin-myosin–based contraction and vesicle-mediated membrane addition. In many cell types, including early *Drosophila* embryos, Nuf/FIP3, a Rab11 effector, mediates recycling endosome (RE)–based vesicle delivery to the cytokinesis furrow. Nuf exhibits a cell cycle–regulated concentration at the centrosome that is accompanied by dramatic changes in its phosphorylation state. Here we demonstrate that maximal phosphorylation of Nuf occurs at prophase, when centrosome-associated Nuf disperses throughout the cytoplasm. Accordingly, ectopic Cdk1 activation results in immediate Nuf dispersal from the centrosome. Screening of candidate kinases reveals a specific, dosage-sensitive interaction between Nuf and Polo with respect to Nuf-mediated furrow formation. Inhibiting Polo activity results in Nuf underphosphorylation and prolonged centrosome association. In vitro, Polo directly binds and is required for Nuf phosphorylation at Ser-225 and Thr-227, matching previous in vivo–mapped phosphorylation sites. These results demonstrate a role for Polo kinase in directly mediating Nuf cell cycle–dependent localization.

INTRODUCTION

Cytokinesis, the final step in mitosis, involves actin-myosin–based ingression of the plasma membrane to produce two distinct daughter cells. Work over the past decade reveals that animal cytokinesis requires a combination of actin-myosin–based contraction and vesicle-mediated membrane delivery. The vesicles, derived from both the secretory and endosomal pathways, provide membrane for the ingressing furrow (Albertson *et al.*, 2005; Schiel and Prekeris, 2013). Functional studies reveal that the recycling endosome (RE) plays a key role in vesicle-based membrane delivery during furrow ingression and abscission, the final stage of cytokinesis (Rothwell *et al.*, 1999). Much of our understanding of the role of the RE in cytokinesis comes from genetic disruption of Rab11, a small GTPase associated with and required for RE function. Disruption of Rab11 results in

specific defects in both the early and late stages of furrow formation (Hickson *et al.*, 2003; Riggs *et al.*, 2003; Fielding *et al.*, 2005; Wilson *et al.*, 2005). RE-derived vesicles deliver key actin regulators and endosomal sorting complex required for transport (ESCRT) proteins to the site of the advancing furrow (Cao *et al.*, 2008; Neto *et al.*, 2013; Schiel and Prekeris, 2013). Thus the RE plays a dual role in providing membrane and in regulating cortical actin dynamics at the advancing furrow.

RE-mediated vesicle delivery to cytokinesis furrows must be precisely coordinated with the cell cycle. Insight into this process comes from the finding that Nuf/FIP3, a Rab11 effector, is necessary for proper RE formation and function and exhibits cell cycle–coordinated changes in its localization and phosphorylation state (Rothwell *et al.*, 1998; Royou *et al.*, 2004; Riggs *et al.*, 2007; Horgan *et al.*, 2010; Otani *et al.*, 2011; Takahashi *et al.*, 2011; Collins *et al.*, 2012). During anaphase in mammalian cells, FIP3 relocalizes from a concentrated centrosomal localization to a diffuse cytoplasmic distribution. FIP3 then accumulates at the furrow and finally during late telophase at the midbody (Takahashi *et al.*, 2011). These changes in subcellular localization are accompanied by changes in the phosphorylation state of FIP3/Nuf (Riggs *et al.*, 2007; Otani *et al.*, 2011). The mechanisms underlying the cell cycle–regulated relocation of FIP3 and the functional significance of the cell cycle–regulated changes in Nuf/FIP3 phosphorylation remain unclear. CDK1-mediated FIP3 phosphorylation sites were identified and mapped.

However, phospho-mutants disrupting these sites had little effect on FIP3 localization or cytokinesis (Otani *et al.*, 2011).

Here we address this issue directly by analyzing Nuf/FIP3 phosphorylation and localization dynamics during the syncytial cortical divisions of the early *Drosophila* embryo. Furrow formation in these rapid divisions is myosin independent and driven primarily by vesicle addition to the plasma membrane (Royou *et al.*, 2004). As in mammalian cells, Rab11 and its Nuf/FIP3 effector are responsible for guiding vesicles originating from the centrosome-associated RE to the ingressing furrow (Rothwell *et al.*, 1999). The RE vesicles contain a potent actin remodeler, RhoGEF, and delivery of these vesicles drives cytoskeletal remodeling at the ingressing furrow (Cao *et al.*, 2008). Unlike conventional cytokinesis, these furrows form during prophase and metaphase and encompass rather than bisect the spindle. Known as metaphase furrows, they are otherwise structurally and compositionally identical to conventional cleavage furrows (Crest *et al.*, 2012).

During interphase through prophase, Nuf associates with and relies on microtubules and the minus-end motor protein dynein to accumulate at the centrosome-associated RE (Riggs *et al.*, 2007). The maximal concentration of Nuf at the centrosome-associated RE correlates with ingression of the metaphase furrows (Riggs *et al.*, 2007). During prophase, Nuf exhibits a dramatic dispersal from the centrosome to the cytoplasm. Like FIP3, Nuf also exhibits cell cycle–

regulated changes in phosphorylation, but the responsible kinases and the functional significance of these phosphorylation events remain unclear.

In the studies presented here, we take advantage of our ability to perform Western blot analysis of individual immunofluorescently stained and imaged *Drosophila* embryos. These studies demonstrate that low and high levels of Nuf phosphorylation correlate with a concentration and dispersal from the centrosome, suggesting a direct involvement of cell cycle–regulated kinases. We use genetic, biochemical, and cell biological techniques to demonstrate that these events are mediated by Polo kinase. We map the Polo-mediated Nuf phosphorylation sites and demonstrate that Polo activity influences Nuf localization at the centrosome.

RESULTS

The cell cycle–regulated dispersal of Nuf from the centrosome is accompanied by increased phosphorylation
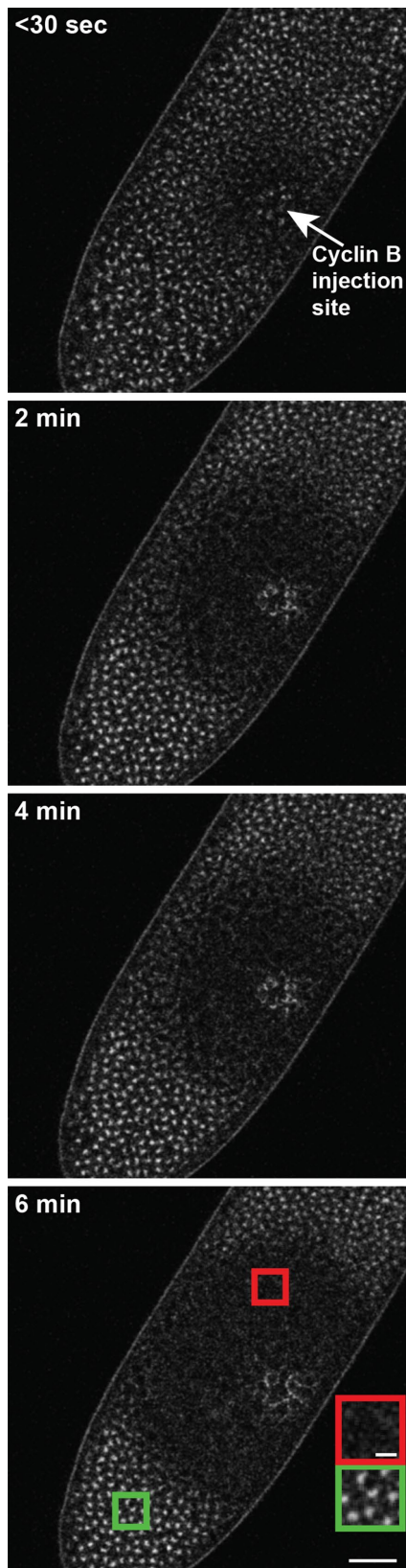
Previous work demonstrated that Nuf protein levels remain constant but undergo cycles of dispersion and concentration at the centrosome that are coordinated with the cell cycle (Rothwell *et al.*, 1998). In addition, these studies demonstrate that Nuf undergoes cell cycle–regulated phosphorylation (Riggs *et al.*, 2007). However, it remained unclear whether highly phosphorylated Nuf was associated with concentration or dispersal from the centrosome. To resolve this issue, we performed Western blot analysis on individual wild-type embryos in which Nuf localization was determined by prior immunofluorescent analysis. The embryos were fixed in the presence of phosphatase and protease inhibitors. After fixation, γ-tubulin (marking the centrosome), Nuf, and DNA were labeled in order to precisely stage and select syncytial nuclear cycle 12 embryos. The distance between sister centrosomes increases as the nuclei progress from early through late interphase (Cao *et al.*, 2010). Thus the separation distance provides a means of precisely timing each embryo and estimating interphase timing based on minutes after nuclear envelope formation at telophase. Once imaged, each embryo was subjected to an ultrasensitive Western blotting technique to determine the phosphorylation state of Nuf (see *Materials and Methods*).

Figure 1A depicts fixed time points in wild-type nuclear cycle 12 embryos as they progress through interphase, prophase, and anaphase. This analysis reveals that Nuf concentration at the centrosome increases during interphase and then abruptly decreases at prophase. As previously described, Western blot analysis reveals a distribution of higher–molecular weight bands corresponding to the phosphorylated Nuf (Rothwell *et al.*, 1998; Riggs *et al.*, 2003; Figure 1B). The single-embryo Western analysis reveals that the intensity of these bands is constant from early through late interphase. However, the intensity of these higher–molecular weight bands dramatically increases
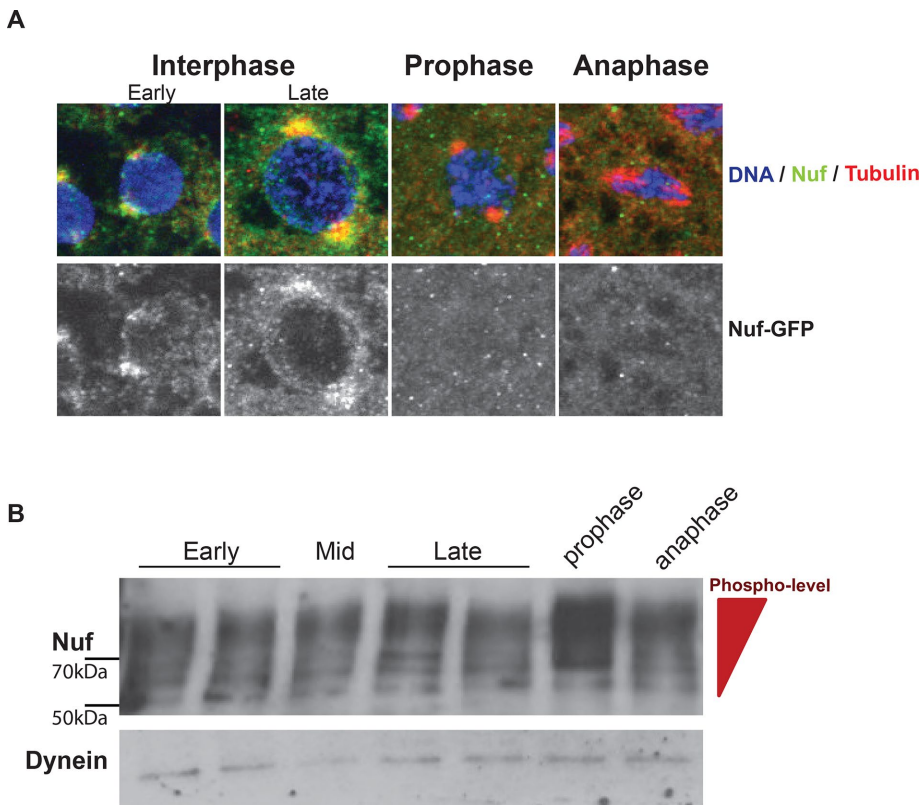
FIGURE 1: Western analysis of single embryos reveals that dispersal of Nuf from the centrosome is correlated with increased phosphorylation. (A) Wild-type cycle 12 embryos, fixed and stained for Nuf (green), tubulin (red), and DNA (blue), reveal that Nuf accumulates at the centrosomes as the embryos progress through interphase. During prophase, Nuf rapidly disperses from the centrosomes to the cytoplasm. (B) Western analysis was performed on individual immunofluorescently stained and imaged embryos. Centrosome distance was used to stage embryos within interphase as described in Cao *et al.* (2010). There is a dramatic increase in the Nuf phosphorylation (higher–molecular weight bands) during prophase concomitant with Nuf dispersal from the centrosomes. Western analysis of dynein served as a loading control.

during prophase. The increase in Nuf phosphorylation is coincident with its dispersal from the centrosome. Thus dispersion of Nuf from the centrosome at prophase is correlated with a dramatic increase in its phosphorylation state.

Cdk1 activation drives a centrosome-to-cytoplasmic relocation of Nuf

The concentration of Nuf at the centrosome during interphase and cytoplasmic dispersal during prophase suggest that cell cycle regulators mediate Nuf localization dynamics. To test this idea, we took advantage of previous studies demonstrating that injection of stabilized cyclin B into interphase syncytial *Drosophila* embryos activates Cdk1 and prematurely drives both the nuclei and cytoplasm into metaphase (Royou *et al.*, 2008). Here we injected stabilized cyclin B into late-interphase cycle 13 syncytial *Drosophila* embryos expressing green fluorescent protein (GFP)–tagged Nuf. At this stage, Nuf is highly concentrated at the centrosomes (Figure 2). These images demonstrate that within 30 s of cyclin B injection, there is a dramatic dispersal of Nuf from the centrosome (Figure 2). As cyclin B radially diffuses from the injection site, there is a corresponding radial dispersal of Nuf from the centrosome over time (Figure 2). The timing and pattern of Nuf dispersal are in accord with previous studies demonstrating injection of stabilized cyclin B driving syncytial nuclei into metaphase (Royou *et al.*, 2008). Significantly, Nuf dispersal occurs only near the injection site, and Nuf remains concentrated at the centrosome in regions distant from the injection site (red and green boxes, respectively). These studies suggest that activation of Cdk1 mediates the centrosome-to-cytoplasmic relocation of Nuf.

A specific, dosage-sensitive interaction between Nuf and Polo kinase

The cyclin B injection studies and cell cycle–dependent phosphorylation states of Nuf suggest that cell cycle–regulated kinases may directly target Nuf. To identify these kinases, we took advantage of previous studies demonstrating that in the early embryo, Nuf exhibits dosage-sensitive phenotypes with actin-remodeling proteins (Cao *et al.*, 2008). Six conserved cell cycle kinases (*bubR1, aur, grp, cdk1, rok, polo*) were screened for a dosage-sensitive interaction with Nuf. Embryos derived from females doubly heterozygous for *nuf* and mutants in one of these six kinases were analyzed for defects in metaphase furrow formation (Rothwell *et al.*, 1998). Figure 3 depicts the results of this analysis. Embryos derived from *nuf¹/+* have no effect on metaphase furrow formation or integrity. Similarly, none of the kinases tested had furrow defects when individually heterozygous in an otherwise wild-type background (*polo, bubR1, aur, grp, cdc2, rok*; unpublished data). Examining embryos derived from females doubly heterozygous for *nuf* and each of the kinase mutants revealed that only *nuf¹/+:polo/+* females produced embryos with disruptions in metaphase furrow formation. Thus, among this set of cell cycle–regulated kinases, Polo is unique in exhibiting a dosage-sensitive interaction with Nuf. This raised the possibility that Polo directly targets Nuf.

FIGURE 2: Cdk1 activation results in a rapid dispersal of Nuf from the centrosome to the cytoplasm. Interphase cycle 13 embryos bearing GFP-Nuf were injected with stabilized GST–cyclin B. At this stage, Nuf is normally concentrated on the centrosomes. Immediately after the injection, Nuf is driven off the centrosomes and dispersed into the cytoplasm. The radius of Nuf dispersal increases over time corresponding to the radial dispersion of the cyclin B, driving Cdk1 activation. The red box indicates an area near the injection site where Nuf is driven off of the centrosome. The green box indicates an area distant from the injection site, where Nuf remains at the centrosome. Scale bars, 50 µm (main image), 10 µm (inset).
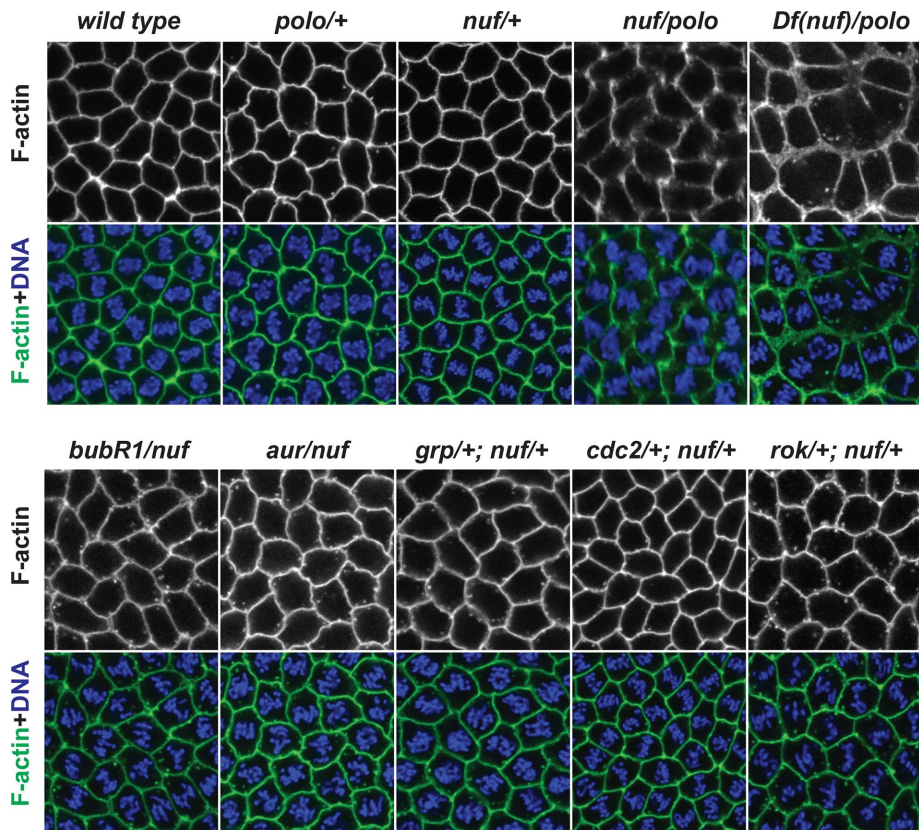
FIGURE 3: Nuf exhibits a dosage-sensitive interaction with Polo kinase. Embryos derived from females doubly heterozygous for *nuf* and one of six cell cycle–regulated kinases (*polo, bubR1, aur, grp, cdk1, rok*) were fixed and stained for their DNA (blue) and actin-based metaphase furrows (green). Only embryos derived from females doubly heterozygous for the *nuf* and *polo* mutants (*nuf¹/+: polo/+*) exhibit defects in the metaphase furrows. The furrows are uneven and weak in places and exhibit gaps. These defects are similar to those observed in embryos derived from *nuf*-homozygous females.

In vivo Nuf phosphorylation sites match in vitro Polo-targeted phosphorylation sites

Pull-down assays demonstrate that Nuf and Polo directly interact. Glutathione-covered Sepharose beads bound with either bacterially purified glutathione *S*-transferase (GST) or GST-Nuf protein were incubated with bacterially expressed MBP-tagged Polo. These beads were then extensively washed, boiled, and run on SDS–PAGE. Western blotting using an anti-MBP antibody detected significant levels of MBP-Polo only in the lane in which the beads were bound with GST-Nuf (Figure 4A). These data demonstrate that Polo kinase physically interacts with Nuf. To test whether Polo kinase mediates Nuf phosphorylation, we performed in vitro kinase assays using baculovirus-expressed Polo (Figure 4C). Polo was incubated with either casein, a known target of Polo, or GST-Nuf in a reaction mix containing [P³³]ATP (see *Materials and Methods*). A mock protein preparation from SF9 cells infected with the virus lacking the Polo gene served as the negative control (Tao *et al.*, 2016). As shown in Figure 4C, casein is highly phosphorylated in these assays, resulting in a band at 30 kDa, demonstrating that the baculovirus-expressed Polo kinase is active in vitro. Of significance, GST-Nuf is also phosphorylated by the same Polo kinase preparation, resulting in a band at 100 kDa. In contrast, the negative control lane failed to reveal phosphorylation of casein or GST-Nuf, indicating that the phosphorylation of Nuf in this assay depends on Polo.

To identify the specific sites on Nuf that Polo phosphorylates, we performed these in vitro assays with and without ATP³². Autoradiography reveals a strong signal at the slowest-migrating, high–molecular weight bands (~100 kDa; Supplemental Figure 1). These bands were excised (asterisks), and liquid chromatography–tandem mass spectrometry (LC MS/MS) was used to identify phosphorylated residues (Supplemental Figure S1). This analysis revealed two amino acids with significant levels of phosphorylation: Ser-225 and Thr-227 (Figure 4D). Significantly, a *Drosophila* genome-wide proteomics study revealed that these same two Nuf residues were phosphorylated in vivo (Zhai *et al.*, 2008).

### Polo inhibition results in decreased Nuf phosphorylation

Taken together, these studies demonstrate that Nuf is likely a direct in vivo target of Polo kinase. To further test this idea, we used a small-molecule inhibitor of polo (BI2536) to reduce its activity in early syncytial embryos and examine the effects on Nuf phosphorylation (Brand and Dormand, 1995). Western blot analysis was performed on 0- to 1.5-h *Drosophila* embryo collections from OreR and *nuf*– mothers, and BI2536 was used to inhibit Polo kinase activity (Figure 5). Anti-Nuf western blots on embryo extracts derived from wild-type (OreR) and homozygous *nuf* females are shown in lanes 1 and 2, respectively, of Figure 5. As previously shown, the higher–molecular weight bands (arrowhead) are the phosphorylated forms of Nuf (Rothwell *et al.*, 1998). The major nonphosphorylated band can be found at 68 kDa (asterisks). These bands are absent in embryo extracts from *nuf*-derived females (lane 2; asterisk indicates where the nonphosphorylated band would be). Extracts from embryos in which Polo activity is reduced through small-molecule inhibition result in a dramatic loss in the abundance of phosphorylated Nuf (lane 3), as seen from the ratio of phosphorylated Nuf to nonphosphorylated Nuf. These studies are in accord with our in vitro experiments and demonstrate an in vivo correlation between Polo activity and Nuf phosphorylation levels, lending additional support to the idea that Nuf is a direct target of Polo kinase both in vitro and in vivo.

Decreased Nuf phosphorylation is correlated with Nuf concentration at the centrosome

Wild-type and OreR embryos treated with the Polo inhibitor BI2536 were fixed and staged as described. During prophase, Nuf reaches its peak concentration at the centrosome. Immunofluorescence analysis of all embryos examined revealed Nuf concentration at the centrosome during prophase (Figure 6). In control embryos, Nuf is absent from the centrosome from prometaphase through telophase. Of interest, the BI2536-treated embryos exhibited maintenance of Nuf at the centrosome through metaphase (Figure 7). Chi-square analysis indicates that BI2536-treated embryos maintain Nuf at the centrosome during metaphase with
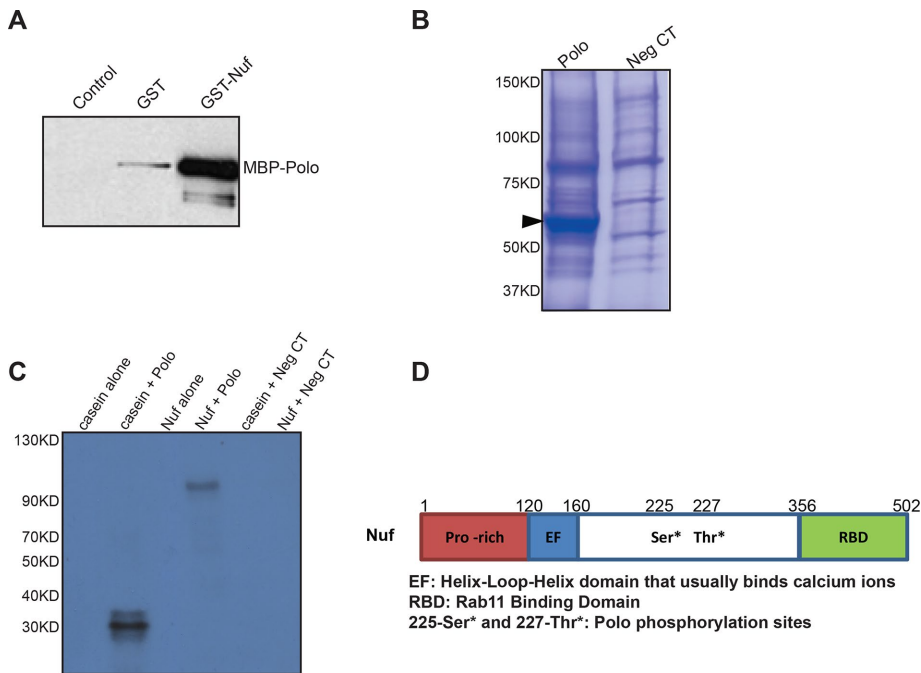
FIGURE 4: Polo directly binds Nuf and is required for Nuf phosphorylation. (A) Pull-down experiments using GST-Nuf and MBP-Polo demonstrate that Nuf directly binds Polo. Bacterially purified GST-Nuf was bound to Sepharose beads. Bacterially purified MBP-Polo was added to the column. Nuf-bound Polo was eluted and probed with MBP antibody on SDS–PAGE. (B) Coomassie stain of baculovirus-expressed Polo and virus without Polo (negative control) illustrates an abundant Polo band (arrowhead) between 50 and 75 kDa not present in the negative control. (C) In vitro assays demonstrate that addition of Polo kinase results in Nuf phosphorylation. Casein was used as positive control. Negative control contains extracts from nontransfected cells. (D) Schematic of Nuf domains, indicating the two residues phosphorylated by Polo as determined by LC MS/MS (unpublished data).
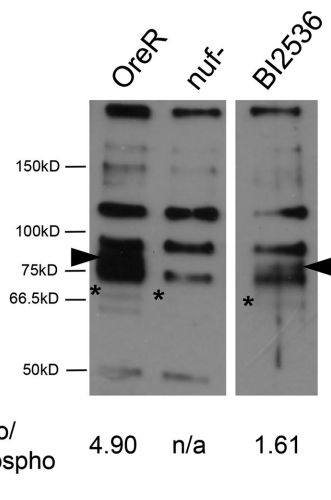
FIGURE 5: Polo inhibition decreases Nuf phosphorylation. Western blot analysis of 0- to 1.5-h embryos reveals the nonphosphorylated band of Nuf at 68kD (asterisks) and the phosphorylated isoforms of Nuf at 82–95 kDa (arrowhead) in wild-type samples. These bands are absent in embryos derived from *nuf* mothers (middle lane). In this lane, the asterisk indicates where the nonphosphorylated band should be. BI2536-treated embryos result in a dramatic decrease in the phosphorylated isoforms (right lane). The calculated ratio of phosphorylated Nuf to nonphosphorylated Nuf indicates a threefold reduction in Nuf phosphorylation when Polo activity is inhibited.

$p = 0.00052$. Embryos of a strong hypomorph of Polo (*polo[10]*) also exhibited this maintenance of Nuf at the centrosome during metaphase (Supplemental Figure S2). Taken together, these data demonstrate that decreased Polo activity results in decreased Nuf phosphorylation and increased association of Nuf with the centrosome.

Of interest, Nuf intensity at the centrosome increases as embryos age, with the lowest intensity measured during cycle 10 and slowly increasing until cellularization (Supplemental Figures S3 and S4). This likely correlates with the lengthening of each nuclear division time, allowing more Nuf to accumulate at the centrosome during later cycles.

DISCUSSION

It is now well documented that the RE plays an important role in vesicle-mediated membrane addition during cytokinesis (Albertson *et al.*, 2005; Montagnac *et al.*, 2008). Less well explored is the spatial and temporal regulation of vesicle-mediated membrane addition. During cytokinesis, the timing of vesicle delivery and actin-myosin–based furrow formation must be precisely coordinated with one another and the cell cycle. Progress on this issue has come from examining the cell cycle dynamics of Rab11, a RE-associated small GTPase, and its effector, FIP3/Nuf. In mammalian cells, Rab11 and FIP3 colocalize and are dispersed throughout the cytoplasm from interphase through metaphase (Takahashi *et al.*, 2011). During anaphase, Rab11/FIP3 predominantly localizes at the pericentrosomal positioned RE. During telophase, Rab11/FIP3 moves from the centrosome to the furrow and then to the midzone microtubules. At the midzone, Rab11/FIP3 is essential for abscission driven by vesicle fusion at the leading edge of the furrow (Horgan *et al.*, 2004; Wilson *et al.*, 2005; Simon and Prekeris, 2008; Simon *et al.*, 2008). This cell cycle–regulated dynamics requires microtubules, as well as motor proteins (Riggs *et al.*, 2003; Horgan *et al.*, 2004).

Taken together, these findings raise a number of issues regarding the relationship between Nuf/FIP3 function, localization, phosphorylation state, and the responsible kinases. Like mammalian FIP3, Nuf undergoes cycles of accumulation at the centrosomes and dispersion throughout the cytoplasm (Rothwell *et al.*, 1998). Nuf concentration at the centrosome-associated RE reaches a maximum at prophase. Entry into metaphase results in a loss of its centrosomal concentration and cytoplasmic dispersion. Previous studies demonstrated that Nuf undergoes cell cycle–regulated phosphorylation, with the highest levels occurring during prophase (Riggs *et al.*, 2007). Here, through a combination of genetic interaction analysis, binding, and kinase assays, we identified Polo kinase as directly targeting Nuf. Among six cell cycle–regulated kinases tested, only Polo exhibited a dosage-sensitive interaction with Nuf. We also found that Polo directly binds Nuf and phosphorylates Nuf in vitro. Significantly, previously mapped in vivo Nuf phosphorylation sites (S225 and T227) match the sites targeted by Polo in our in vitro
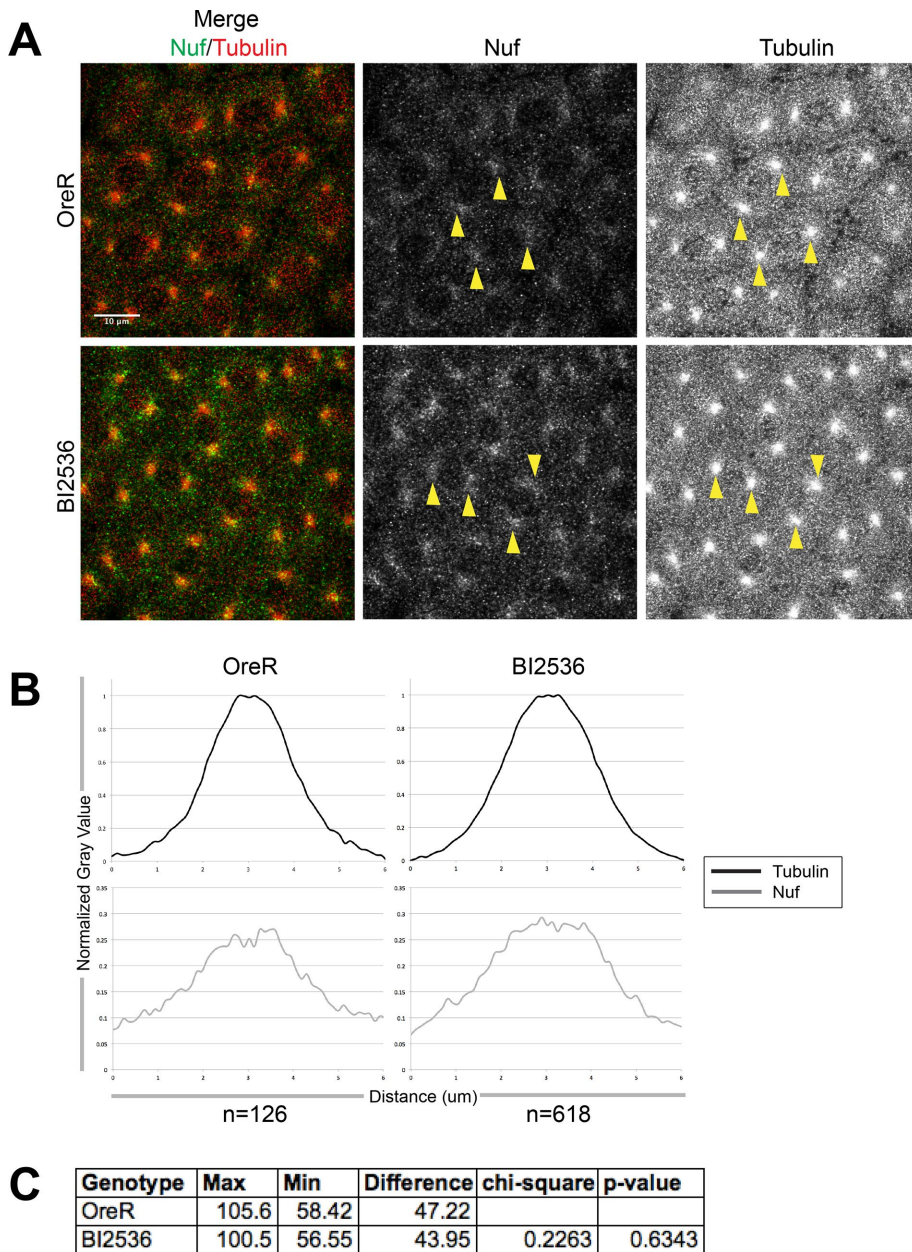
FIGURE 6: Polo inhibition does not change Nuf localization during prophase. (A) Untreated (top) and BI2536 (Polo inhibitor)-treated (bottom) prophase cycle 11 embryos stained for Nuf (green) and tubulin (red). Arrowheads indicate the position of the centrosome in both the tubulin and Nuf channels. (B) Nuf (gray) and tubulin (black) intensity at the centrosome for each genotype at cycles 11 and 12, where 3 represents the center of the centrosome. The values are normalized to tubulin signal (0–1), and the axes for Nuf graphs are expanded to compare the two treatments. *OreR*, n = 126; BI2536, n = 618. (C) Highest average Nuf intensity, lowest average Nuf intensity, and difference between these intensities for all cycle 11 and 12 embryos for each treatment, as well as the chi-square value (as compared with *OreR*) and corresponding p value. All analyses were performed on the raw data.

tion, Polo has emerged as a key regulator of cytokinesis, controlling both the timing and position of furrow formation, as well as membrane addition (Ohkura *et al.*, 1995; Herrmann *et al.*, 1998). The positioning of these residues is not conserved from Nuf to FIP3, suggesting that phosphorylation of other sequences in FIP3 is required to effect its localization in mammalian cells.

To determine the functional consequences of Polo-mediated phosphorylation of Nuf, we examined the timing of Nuf centrosomal localization when Polo activity is inhibited by the small molecule BI2536. In wild-type syncytial embryos, Nuf concentrates at the centrosome during interphase through prophase and is released into the cytoplasm at prophase, marked by nuclear envelope breakdown (NEB). Embryos treated with the small-molecule inhibitor of Polo, BI2536, exhibit wild-type behavior during interphase through prophase, but the release of Nuf into the cytoplasm is significantly delayed, and Nuf remains concentrated at the centrosome well after NEB. Taken together, these results demonstrate a role for Polo kinase in directly mediating Nuf cell cycle–dependent localization.

The mechanism mediating Nuf release from the centrosome remains unclear. High-resolution live studies demonstrate vectorial transport of individual Nuf puncta, suggesting that this may rely on microtubules and an as-yet-unidentified kinesin (Riggs *et al.*, 2007). This notion is in accord with studies demonstrating that the organization and positioning of other endosomes is driven by a combination of plus and minus end–directed motor proteins (Pangarkar *et al.*, 2005). A recent study showed that perturbation of both Nuf and dynein negatively affect the recruitment of Cad99C to the apical end of microvilli in *Drosophila* epithelial cells, suggesting that Nuf and dynein work together when moving Rab11 vesicles toward microtubule minus ends (Khanal *et al.*, 2016). Nuf physically associates with dynein and requires this minus-end motor protein for proper recruitment to the centrosome (Horgan *et al.*, 2004; Riggs *et al.*, 2007). A previous study observed directional movement of Nuf away from the centrosome during live analysis, suggesting that Nuf may rely on the plus end–directed motor kinesin when it is released from the centrosome (Riggs *et al.*, 2003).

Insight into the mechanism by which Polo-mediated phosphorylation of Nuf influences its recruitment to the centrosome comes from previous studies of Nlp. Nlp is a centrosomal protein that recruits γ-tubulin and plays an important role in early centrosome maturation; Nlp also localizes to the centrosome via its interaction with dynein (Casenghi *et al.*, 2005). Phosphorylation by Polo causes
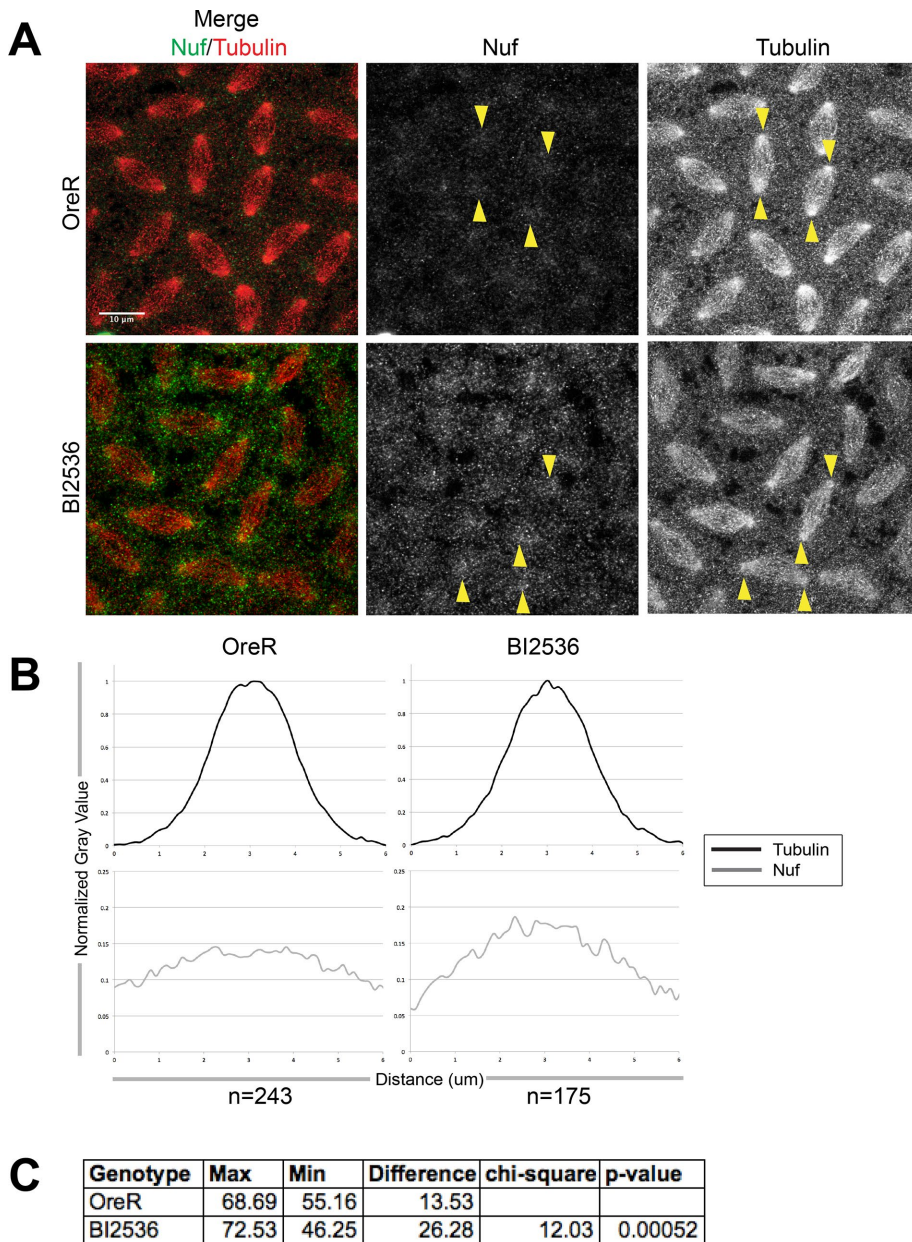
kinase assays (Zhai *et al.*, 2008). These findings are supported by our in vivo studies indicating that decreased Polo activity results in corresponding decreases in Nuf phosphorylation. Previous studies demonstrated that Polo localizes to the centrosome during prophase, which corresponds to the time of maximal Nuf centrosomal concentration (Moutinho-Santos *et al.*, 1999). Therefore Polo is well positioned to influence the phosphorylation state of Nuf. In addi-

FIGURE 7: Polo inhibition results in Nuf maintenance at the centrosome during metaphase. (A) Untreated (top) and BI2536 (Polo-inhibitor)-treated (bottom) prophase cycle 11 embryos stained for Nuf (green) and tubulin (red). Arrowheads indicate the position of the centrosome in both the tubulin and Nuf channels. (B) Nuf (gray) and tubulin (black) intensity at the centrosome for each genotype at cycles 11 and 12, where 3 represents the center of the centrosome. The values are normalized to tubulin signal (0–1), and the axes for Nuf graphs are expanded to compare the two treatments. *OreR*, $n = 243$; BI2536, $n = 175$. (C) Highest average Nuf intensity, lowest average Nuf intensity, and difference between these intensities for all cycle 11 and 12 embryos for each treatment, as well as the chi-square value (as compared with *OreR*) and corresponding p value. All analyses were performed on the raw data.

Nlp to lose its binding to dynein, and accumulation is rapidly lost. Based on these studies, we speculate that Polo phosphorylation disrupts Nuf's ability to associate with dynein. This disruption would inhibit dynein-mediated recruitment of Nuf to the centrosome and result in the observed cytoplasmic dispersion of Nuf at prophase. Of interest, a study found that in hair follicle–producing cells in *Drosophila*, Nuf trafficking of RE vesicles was directly regulated by IKK kinase, which phosphorylates Nuf and affects its association

with dynein (Otani *et al.*, 2011). Moreover, that phosphorylation was at S225, one of the sites found in our studies. In both *Drosophila* and HEK293 cells, Nuf/FIP3 is phosphorylated by the IKK-related kinases IKKε and TBK1 (Otani *et al.*, 2011).

Other studies found the FIP3 residue S102 to be directly phosphorylated by Cdk1-cyclin B (Collins *et al.*, 2012). These studies indicate that Nuf/FIP3 is targeted by a number of kinases and at multiple sites that may affect its interaction with other proteins. Our data implicate Polo as the primary kinase responsible for Nuf dissociation from the centrosome in the early *Drosophila* embryo. The residues surrounding S225 and T227 that we identified do not conform to the traditional consensus sequence for Polo binding, suggesting that we discovered a novel targeting site for Polo kinase (Elia *et al.*, 2003).

These studies were performed in the early *Drosophila* embryo, in which cytokinesis furrows encompass rather than bisect the spindle and RE-mediated vesicle addition occurs from the centrosome rather than the midzone (Crest *et al.*, 2012). In conventional cytokinesis, FIP3/Rab11 localizes to the midzone microtubules to activate RE-mediated vesicle delivery during the final abscission stages of cytokinesis (Takahashi *et al.*, 2011). Like Nuf, FIP3 undergoes cell cycle–regulated phosphorylation events. Given our results and the fact that Polo kinase concentrates at the midzone microtubules, we suspect Polo may be a key kinase that targets and influences FIP3 localization at the midzone in mammalian cells (Moutinho-Santos *et al.*, 1999). A full understanding of the role of phosphorylation in the cell cycle regulation of Nuf localization requires the construction of phosphomimetic and non-phosphorylatable Nuf transgenic lines. This will be a focus of our future studies.

MATERIALS AND METHODS

Fly strains
Stocks were maintained on standard maize meal/molasses medium at room temperature unless otherwise noted. *OreR* served as the wild-type control stock. Other stocks used in this study include Nuf1/TM3, Sb (Rothwell *et al.*, 1999), polo10/TM6C, Tb, Sb (Bloomington), GFP-Nuf/CyO (Riggs *et al.*, 2003), alphaTub-Gal4:VP16 (Bloomington), Sqh-GFP (Royou *et al.*, 2004), and Moesin-GFP (Cao *et al.*, 2008).

Embryo fixation and immunostaining
Flies laid eggs for 1 h at 29°C, and then embryos were aged for 1 h at room temperature. Collected embryos were dechorionated in 50% bleach for 2 min, extensively rinsed, permeabilized in heptane, and transferred into a mixture with equal volume of heptane

and 37% formaldehyde for 5 min. The formaldehyde was removed, and the embryos were devitellinated in a 1:1 solution of heptane and methanol for 1 min. The heptane was removed, and the embryos were stored in methanol at 4°C. The embryos were rehydrated in PBTA (phosphate-buffered saline [PBS] + 0.1% Triton X-100 + 0.05% sodium azide) before staining. The primary antibodies used include rabbit anti-Nuf (1:250; Rothwell et al., 1999), rabbit anti-pNuf S225 (1:30; Otani et al., 2011), and mouse anti-tubulin DM1A (1:100; 9020; Sigma-Aldrich). Secondary Alexa 488- and 594–conjugated antibodies were used at 1:300 or 1:500 (Molecular Probes).

Single-embryo Western immunoblots
Immunoblots of staged embryos were prepared as previously described (Riggs et al., 2007). Collected embryos were dechorionated in 50% bleach for 2 min, extensively rinsed, permeabilized in heptane, and transferred into a mixture with equal volume of heptane and methanol (containing 1 mM Na_3VO_4) for fixation. Embryos were rinsed three times in ice-cold 99% methanol with 1 mM Na_3VO_4 and rehydrated with embryo buffer (EB) containing 10 mM of NaF. The embryos were then stained with EB containing 4 μg/ml Hoechst 33258 for 3–4 min, rinsed twice in EB, and transferred to 40% EB/60% glycerol. Embryos were staged visually using the 4′,6-diamidino-2-phenylindole channel of a fluorescent microscope. Hand-picked cycle 13 embryos (four per sample) were dissolved in 2Å~ SDS sample buffer and run on SDS–PAGE and immunoblotting using standard procedures.

Multiple-embryo Western immunoblots
Embryos were collected from OreR and nuf embryos after lying for 1.5 h at room temperature. Embryos were hand dechorionated and lysed directly in 25 μl of 1× SDS sample buffer. Each sample contained 15 embryos from each genotype. Samples were stored at –80°C. Samples were thawed, spun down, and boiled for 10 min, and then 20 μl was loaded onto a 7.5% precast SDS gel (Bio-Rad), which was run at 100 V for 80 min. The protein was transferred to nitrocellulose at 100 V for 1 h at 4°C. The membrane was Ponceau stained to confirm proper transfer and then blocked for 30 min in 5% dry milk plus PBS-Tween (PBS-T) at room temperature. The membrane was incubated with primary overnight at 4°C (rabbit anti-Nuf, 1:750). The membrane was rinsed 3 × 10 min in PBS-T at room temperature and then incubated in secondary for 1.5 h at room temperature (goat anti-rabbit horseradish peroxidase, 1:5000). The membrane was rinsed 3 × 10 min in PBS-T at room temperature and then treated with visualization solution (ThermoSci SuperSignal West Pico Chemiluminescent Substrate). Optimum exposure time was 5 min on film. Quantification of these bands was performed using Fiji.

Treatment of embryos with BI2536
Embryos were collected for fixing and staining or Western blot analysis as described. For Western blot analysis, OreR embryos were hand dechorionated and then placed in a tube with a 1:1 solution of heptane and 1 μM BI2536 (in dimethyl sulfoxide [DMSO]; Santa Cruz Biotechnology) and vigorously mixed every 2 min for 10 min (about the length of a single cell cycle). The DMSO layer was removed, and then the embryos were removed from the heptane to dry. Each of 15 embryos was lysed in SDS loading buffer and subjected to SDS–PAGE analysis as described. As a control, OreR embryos were also treated in a 1:1 solution of heptane and DMSO.

For fixing and staining, OreR embryos were collected as described. After bleach dechorionation, the embryos were permeabilized in a 1:1 solution of heptane and 1 μM BI2536 and vigorously

mixed every 2 min for 10 min. The DMSO layer was removed, and the rest of the fix and stain procedure followed the described protocol. As a control, OreR embryos were also treated in a 1:1 solution of heptane and DMSO.

Kinase assay
Full-length Polo kinase cDNA was cloned into a Gateway baculovirus expression construct (Invitrogen) with a hexahistidine (6×His) tag. Sf9 cells were infected and then harvested on a nickel column at a concentration of 0.5 mg/ml. GST-tagged Nuf (Rothwell et al., 1999) was purified using glutathione–Sepharose beads to a concentration of 1 mg/ml. Dephosphorylated casein (Sigma-Aldrich) was dissolved in water to 1 mg/ml. Kinase reactions were assembled using 5 μg of substrate (casein or GST-Nuf), 0.05 mM ATP, 0.05 μg of Polo-6×His, 5 μCi of ATP32, and kinase buffer (10 mM 4-(2-hydroxyethyl)-1-piperazineethanesulfonic acid, pH 7.5, 75 mM KCl, 5 mM $MgCl_2$, 1 mM dithiothreitol, 0.5 mM ethylene glycol tetraacetic acid). Extracts from Sf9 cells infected with empty virus were used as control kinases at 0.5 mg/ml. The 25-μl reactions were carried out at 30°C for 20 min and then boiled in 2× sample buffer and run on SDS–PAGE. Nonradiolabeled Polo phosphorylated bands were gel extracted and used for tandem mass spectrometry. Mass spectrometry was performed by the Bio-Organic Biomedical Mass Spectrometry Resource at the University of California, San Francisco, using standard protocols.

Confocal microscopy and image analysis
Confocal microscope images were captured on an inverted photoscope (DMIRB; Leitz) equipped with a laser confocal imaging system (TCS SP2; Leica) using an HCX PL APO 63×/numerical aperture 1.4 oil objective (Leica) at room temperature.

The images in Figures 6 and 7 were edited in exactly the same way with minor adjustments to brightness and contrast to emphasize the localization. All fixed images were quantified using Fiji software using the raw files. For each image, a 6-μm line was drawn through the center of each centrosome tangent to the nucleus, and pixel intensity was measured along the line in both tubulin and Nuf channels. In Excel, the pixel intensity for each centrosome was averaged for each embryo. To combine embryo data of the same genotype and cell cycle stage, the average values for each embryo were scaled with respect to the peak tubulin value of the highest embryo such that each embryo would have the same intensity for the peak tubulin value. These adjusted averages were then averaged again. The graphs represent the pixel intensity for both the Nuf and tubulin channels normalized to the tubulin signals (0 = lowest tubulin value; 1 = highest tubulin value). For chi-square analysis, the lowest average Nuf value (from all cycle 11 and 12 embryos) was subtracted from the peak average Nuf value to find the difference. The difference was then subjected to chi-square analysis, where OreR represents the "expected" value.

Supplemental Figure S2 was captured live after injection of rhodamine-labeled tubulin (Cytoskeleton) into cycle 11 GFP Nuf or GFP Nuf; $polo^{10}$ embryos.

REFERENCES

Albertson R, Riggs B, Sullivan W (2005). Membrane traffic: a driving force in cytokinesis. Trends Cell Biol 15, 92–101.

Brand AH, Dormand EL (1995). The GAL4 system as a tool for unravelling the mysteries of the Drosophila nervous system. Curr Opin Neurobiol 5, 572–578.

Cao J, Albertson R, Riggs B, Field CM, Sullivan W (2008). Nuf, a Rab11 effector, maintains cytokinetic furrow integrity by promoting local actin polymerization. J Cell Biol 182, 301–313.

Cao J, Crest J, Fasulo B, Sullivan W (2010). Cortical actin dynamics facilitate early-stage centrosome separation. Curr Biol 20, 770–776.

Casenghi M, Barr FA, Nigg EA (2005). Phosphorylation of Nlp by Plk1 negatively regulates its dynein-dynactin-dependent targeting to the centrosome. J Cell Sci 118, 5101–5108.

Collins LL, Simon G, Matheson J, Wu C, Miller MC, Otani T, Yu X, Hayashi S, Prekeris R, Gould GW (2012). Rab11-FIP3 is a cell cycle-regulated phosphoprotein. BMC Cell Biol 13, 4.

Crest J, Concha-Moore K, Sullivan W (2012). RhoGEF and positioning of rappaport-like furrows in the early Drosophila embryo. Cur Biol 22, 2037–2041.

Elia AE, Rellos P, Haire LF, Chao JW, Ivins FJ, Hoepker K, Mohammad D, Cantley LC, Smerdon SJ, Yaffe MB (2003). The molecular basis for phosphodependent substrate targeting and regulation of Plks by the Polo-box domain. Cell 115, 83–95.

Fielding AB, Schonteich E, Matheson J, Wilson G, Yu X, Hickson GR, Srivastava S, Baldwin SA, Prekeris R, Gould GW (2005). Rab11-FIP3 and FIP4 interact with Arf6 and the exocyst to control membrane traffic in cytokinesis. EMBO J 24, 3389–3399.

Herrmann S, Amorim I, Sunkel CE (1998). The POLO kinase is required at multiple stages during spermatogenesis in Drosophila melanogaster. Chromosoma 107, 440–451.

Hickson GR, Matheson J, Riggs B, Maier VH, Fielding AB, Prekeris R, Sullivan W, Barr FA, Gould GW (2003). Arfophilins are dual Arf/Rab 11 binding proteins that regulate recycling endosome distribution and are related to Drosophila nuclear fallout. Mol Biol Cell 14, 2908–2920.

Horgan CP, Hanscom SR, Jolly RS, Futter CE, McCaffrey MW (2010). Rab11-FIP3 binds dynein light intermediate chain 2 and its overexpression fragments the Golgi complex. Biochem Biophys Res Commun 394, 387–392.

Horgan CP, Walsh M, Zurawski TH, McCaffrey MW (2004). Rab11-FIP3 localises to a Rab11-positive pericentrosomal compartment during interphase and to the cleavage furrow during cytokinesis. Biochem Biophys Res Commun 319, 83–94.

Khanal I, Elbediwy A, Diaz de la Loza Mdel C, Fletcher GC, Thompson BJ (2016). Shot and Patronin polarise microtubules to direct membrane traffic and biogenesis of microvilli in epithelia. J Cell Sci 129, 2651–2659.

Montagnac G, Echard A, Chavrier P (2008). Endocytic traffic in animal cell cytokinesis. Curr Opin Cell Biol 20, 454–461.

Moutinho-Santos T, Sampaio P, Amorim I, Costa M, Sunkel CE (1999). In vivo localisation of the mitotic POLO kinase shows a highly dynamic association with the mitotic apparatus during early embryogenesis in Drosophila. Biol Cell 91, 585–596.

Neto H, Balmer G, Gould G (2013). Exocyst proteins in cytokinesis: regulation by Rab11. Commun Integr Biol 6, e27635.

Ohkura H, Hagan IM, Glover DM (1995). The conserved Schizosaccharomyces pombe kinase plo1, required to form a bipolar spindle, the actin ring, and septum, can drive septum formation in G1 and G2 cells. Genes Dev 9, 1059–1073.

Otani T, Oshima K, Onishi S, Takeda M, Shinmyozu K, Yonemura S, Hayashi S (2011). IKKepsilon regulates cell elongation through recycling endosome shuttling. Dev Cell 20, 219–232.

Pangarkar C, Dinh AT, Mitragotri S (2005). Dynamics and spatial organization of endosomes in mammalian cells. Phys Rev Lett 95, 158101.

Riggs B, Fasulo B, Royou A, Mische S, Cao J, Hays TS, Sullivan W (2007). The concentration of Nuf, a Rab11 effector, at the microtubule-organizing center is cell cycle-regulated, dynein-dependent, and coincides with furrow formation. Mol Biol Cell 18, 3313–3322.

Riggs B, Rothwell W, Mische S, Hickson GR, Matheson J, Hays TS, Gould GW, Sullivan W (2003). Actin cytoskeleton remodeling during early Drosophila furrow formation requires recycling endosomal components Nuclear-fallout and Rab11. J Cell Biol 163, 143–154.

Rothwell WF, Fogarty P, Field CM, Sullivan W (1998). Nuclear-fallout, a Drosophila protein that cycles from the cytoplasm to the centrosomes, regulates cortical microfilament organization. Development 125, 1295–1303.

Rothwell WF, Zhang CX, Zelano C, Hsieh TS, Sullivan W (1999). The Drosophila centrosomal protein Nuf is required for recruiting Dah, a membrane associated protein, to furrows in the early embryo. J Cell Sci 112, 2885–2893.

Royou A, Field C, Sisson JC, Sullivan W, Karess R (2004). Reassessing the role and dynamics of nonmuscle myosin II during furrow formation in early Drosophila embryos. Mol Biol Cell 15, 838–850.

Royou A, McCusker D, Kellogg DR, Sullivan W (2008). Grapes(Chk1) prevents nuclear CDK1 activation by delaying cyclin B nuclear accumulation. J Cell Biol 183, 63–75.

Schiel JA, Prekeris R (2013). Membrane dynamics during cytokinesis. Curr Opin Cell Biol 25, 92–98.

Simon GC, Prekeris R (2008). Mechanisms regulating targeting of recycling endosomes to the cleavage furrow during cytokinesis. Biochem Soc Trans 36, 391–394.

Simon GC, Schonteich E, Wu CC, Piekny A, Ekiert D, Yu X, Gould GW, Glotzer M, Prekeris R (2008). Sequential Cyk-4 binding to ECT2 and FIP3 regulates cleavage furrow ingression and abscission during cytokinesis. EMBO J 27, 1791–1803.

Sommi P, Ananthakrishnan R, Cheerambathur DK, Kwon M, Morales-Mulia S, Brust-Mascher I, Mogilner A (2010). A mitotic kinesin-6, Pav-KLP, mediates interdependent cortical reorganization and spindle dynamics in Drosophila embryos. J Cell Sci 123, 1862–1872.

Takahashi S, Takei T, Koga H, Takatsu H, Shin HW, Nakayama K (2011). Distinct roles of Rab11 and Arf6 in the regulation of Rab11-FIP3/arfophilin-1 localization in mitotic cells. Genes Cells 16, 938–950.

Tao L, Fasulo B, Warecki B, Sullivan W (2016). Tum/RacGAP functions as a switch activating the Pav/kinesin-6 motor. Nat Commun 7, 11182.

Wilson GM, Fielding AB, Simon GC, Yu X, Andrews PD, Hames RS, Frey AM, Peden AA, Gould GW, Prekeris R (2005). The FIP3-Rab11 protein complex regulates recycling endosome targeting to the cleavage furrow during late cytokinesis. Mol Biol Cell 16, 849–860.

Zhai B, Villen J, Beausoleil S, Mintseris J, Gygi S (2008). Phosphoproteome analysis of Drosophila melanogaster embryos. J Proteome Res 7, 1675–1682.